Neuromodulation: Technology at the Neural Interface

Received: March 20, 2025 Revised: August 9, 2025 Accepted: August 27, 2025

https://doi.org/10.1016/j.neurom.2025.08.414

# Distinct Patterns of Temporally Coded Electrical Stimulation Interfere With Long-Range Interhemispheric Coupling in a Focal Model of Epilepsy

Larissa Samara Santos Xavier, MSc<sup>1</sup>; Thiago Moreira Maia Montalvão, MSc<sup>1</sup>; Leonardo de Oliveira Guarnieri, PhD<sup>1,3</sup>; João Pedro Carvalho-Moreira, PhD<sup>1,3</sup>; Matheus Costa Passos, BSc<sup>1</sup>; Vinícius Rosa Cota, PhD<sup>2</sup>; Márcio Flávio Dutra Moraes, PhD<sup>1</sup> ©

#### **ABSTRACT**

**Objectives:** This study investigated 1) epileptiform activity propagation triggered by intrahippocampal kainic acid (KA) injections, 2) whether low-frequency probing stimulation applied to the ipsilateral amygdaloid complex (AMY) would affect propagation, and 3) whether distinct temporal patterns of electrical stimulation applied to the contralateral amygdaloid complex interfere with the interhemispheric propagation pattern.

Materials and Methods: Electrical stimulation (ES) comprised a 100-μs pulse of 500 μA applied to the AMY. The Probing protocol applied a 2000-millisecond interpulse-interval (IPI) ES ipsilateral to KA injection. The Propagation protocol ES was applied contralateral to KA injection using temporally coded ES patterns: periodic stimulation (PS, with fixed 250-millisecond IPI or nonperiodic stimulation [NPS], power-law distributed IPIs constrained by a maximum of 4 pulses/s). Continuous local-field electrophysiologic data were recorded from AMY and hippocampus sites in both hemispheres.

**Results:** Our results show that probing stimulation to the ipsilateral amygdala does not interfere with the seizure propagation pattern; however, independent contralateral seizures were observed. Our data show that NPS treatment, but not PS, interferes with propagation to the contralateral hemisphere even when applied before KA injection: seizure duration, energy, and total number of seizures were significantly reduced. Seizure causality analysis between channels also shows significant differences between PS and NPS treatments.

**Conclusion:** These data corroborate that KA injection seizures, even during status epilepticus, are not restricted to injection foci. Our data show promising perspectives on designing a closed-loop solution using 0.5-Hz probing stimulation to predict seizures and temporally coded stimulation to modulate seizure propagation.

**Keywords:** Closed-loop, DBS—deep brain electrical stimulation, epilepsy, neuromodulation, seizure control, seizure prediction, seizure propagation

Address correspondence to: Márcio Flávio Dutra Moraes, PhD, Núcleo de Neurociências, Departamento de Fisiologia e Biofísica, Instituto de Ciências Biológicas - Universidade Federal de Minas Gerais, Av. Antônio Carlos, 6627 - CEP 31270-901- Campus Pampulha, Belo Horizonte MG, Brazil. Email: mfdm@icb.ufmg.br

For more information on author guidelines, an explanation of our peer review process, and conflict of interest informed consent policies, please see the journal's Guide for Authors.

Source(s) of financial support: The following funding agencies supported this work: FAPEMIG APQ-03295-18, CNPq 405419/2021-0, CNPq 309428/2021-1, CNPq 408170/2023-9, Leamman Foundation, and CAPES. Márcio Flávio Dutra Moraes is supported by a fellowship from CNPq.

<sup>&</sup>lt;sup>1</sup> Department of Physiology and Biophysics, Núcleo de Neurociências, Federal University of Minas Gerais, Belo Horizonte, Brazil;

<sup>&</sup>lt;sup>2</sup> Department of Electronic Engineering, Maynooth University, Maynooth, Ireland; and

<sup>&</sup>lt;sup>3</sup> Centro de Tecnologia e Pesquisa em Magneto Ressonância, Programa de Pós-Graduação em Engenharia Elétrica—Universidade Federal de Minas Gerais, Belo Horizonte, Brasil

# INTRODUCTION

Despite decades of scientific advancements, epilepsy continues to represent a significant global health burden, affecting the lives of patients, families, and society.<sup>1</sup> Notwithstanding the high prevalence of the disease, which affects 1% to 2% of the population worldwide,<sup>2</sup> current first-line treatments often fail to provide full relief of seizures and associated symptoms. Although antiepileptic drugs manage to control seizures in only approximately 70% of patients,<sup>3</sup> surgical intervention—an option primarily for refractory cases—is feasible in fewer than half of such instances.<sup>4</sup> Even in those cases, the surgery removes brain tissue in hopes that neither function would be severely compromised, nor is an alternate route for seizure propagation and/or genesis eventually likely to evolve.<sup>5</sup> In contrast, the pharmacologic approach to treatment often aims to change the state of the system, maintaining constant tonic modulation, rather than acting at specific time windows that may alter system dynamics, that is, interfering precisely when the system is becoming unstable.<sup>6-9</sup> This traditional perspective—targeting constant network activity inhibition through neurochemical agents or surgically excising dysfunctional regions—may be the reason there has been little advance in new therapeutic strategies that can resolve cases that have been unsuccessful using conventional available therapies.<sup>3,6–9</sup> Ideally, closed-loop solutions, such as the Food and Drug Administration (FDA)-approved NeuroPace RNS System<sup>®, 8,9</sup> offer a promising alternative by approaching the disease from two key angles: 1) acquisition of data that may be used to provide a reliable indication that network activity is shifting toward instability (ie, seizure prediction)<sup>10–13</sup> and 2) delivering precise, fast-acting neuromodulation to restore stability to network dynamics. 14,15 Implementing this strategy, openloop neuromodulation techniques approved by the FDA, such as deep brain stimulation (DBS) and vagus nerve stimulation have consistently shown therapeutic effects in preclinical and clinical trials 16 by suppressing or attenuating seizures while also putatively inducing plasticity and curative brain rewiring.<sup>17</sup> Although highly promising, the complex neurophysics underlying the interactions between electromagnetic fields and the intricate cytoarchitectonic structure of neural tissue still represents a major obstacle to fully understanding the mechanisms underlying therapeutic efficacy. 18 This jeopardizes the design of more robust, efficient, and safe neuromodulation methods. 12,19,20

Further advancements in the field must prioritize mechanistic insight over pure empiricism.<sup>21–23</sup> In this context, the modern framework for brain architecture based on the role of neural synchronism in long-range integration and signal processing has proved invaluable.<sup>24–27</sup> Neural synchronization, described as the driving interaction between oscillatory systems<sup>28</sup>—brain structures in this case—manifests across multiple organizational levels. It spans from the molecular processes of coincidence detection in the synapse that lead to neuroplasticity, <sup>29</sup> to neural network dynamics responsible for the origin of major electrographic oscillations,<sup>24</sup> including global long-range brain integration that underlies both major cognitive processes  $^{26}$  and fundamental circadian rhythms (eg, sleep-wake cycle).  $^{30-32}$  As the dysfunctional side of the same coin, aberrant synchronism is a hallmark of many neurologic disorders.<sup>33,34</sup> In epilepsy, excessive neural synchronism is intricately linked to distinct epileptic phenomena, including maladaptive plasticity underlying epileptogenesis (and kindling),<sup>35</sup> abnormal neuronal coupling that contributes to hyperexcitability,<sup>36</sup> the circuit-level mechanisms driving seizure activity (ictogenesis).<sup>6,37–39</sup> It also plays a key role in propagating epileptiform activity across distant brain areas.<sup>40–42</sup> Notably, neural synchronism mediated by a myriad of structures, including neural hubs in subcortical regions and the corpus callosum, has been recognized as a central mechanism of interhemispheric generalization of primarily partial seizures.<sup>43–47</sup>

Viewing neurologic disorders as dysfunctions of neural synchronism has allowed in-depth understanding of neurobiology in addition to the proposition of novel therapeutic approaches.<sup>22</sup> In particular, the rationale of designing electrical stimulation methods specifically tailored to modulate synchronization levels across brain structures holds great promise. In 2009, our group showed that seizures in animal models could be modulated according to the temporal regularity of pulsatile stimulation.<sup>22</sup> Specifically, although periodic low-frequency (4 Hz) electrical stimulation of the basolateral amygdala precipitated convulsive behaviors related to the recruitment of mesial temporal lobe seizures, nonperiodic stimuli (with IPIs following a power-law distribution) of equal average frequency (4 pulses/s) robustly delayed the occurrence of behaviors originating from both partial and generalized epileptiform activity. This anticonvulsant effect of nonperiodic stimulation (a stimulus later termed NPS) was repeatedly indicated in acute and chronic seizures. 11,12,14,48-51 Mechanistic investigations indicated that long-range synchronismmodulating effects mediated by the amygdala might have a preponderant role. 14,48,52 The amygdala has been extensively described as a neural hub of major importance not only in mediating various brain functions<sup>53,54</sup> but also in supporting epileptic phenomena, including ictogenesis,<sup>55</sup> seizure propagation,<sup>56</sup> status epilepticus,<sup>57</sup> and kindling.<sup>58,59</sup>

In this study, we investigated the propagation pattern of epileptiform activity triggered by focal intrahippocampal injections of kainic acid (KA) during the status epilepticus. Moreover, we explored two hypotheses central to the closed-loop approach to epilepsy therapy: 1) Low-frequency (0.5 Hz), low-amplitude stimulation ipsilateral to the KA injection does not significantly affect seizure severity or propagation; this suggests that such stimulation parameters could be used for seizure prediction without interfering with seizure dynamics; and 2) temporal patterns of amygdala stimulation—periodic stimulation (PS, fixed frequency) vs temporally complex and irregular stimulation (NPS)—differentially influence the interhemispheric long-range propagation of seizures induced by contralateral intrahippocampal KA injection. Specifically, we predicted that PS would favor the propagation of seizures to the hemisphere contralateral to the onset region, whereas NPS would impair it. The rationale follows the framework described in previous work, in which the amygdala, as a major brain hub for transferring activity across the brain, recruits distinct areas according to the temporal regularity of said activity. Thus, we have previously established that electrically stimulating the amygdaloid complex with different temporal patterns can be used to predict seizure occurance, 10,11 facilitate seizures, and/or attenuate seizures 14,48,50,52,60 in animal models of epilepsy. In this sense, regular oscillation, such as those from PS, would promote the formation of reverberant (thus ictogenic) circuits that facilitate seizure propagation. At the same time, temporally complex, NPS would disrupt network integration, impairing seizure generalization. Accordingly, low-frequency/low-amplitude stimuli to the ipsilateral amygdala should not interfere with ictogenesis or seizure propagation, thus making it suitable for seizure prediction.

# **MATERIALS AND METHODS**

### **Animals and Experimental Design**

This work was conducted using male Wistar Hannover rats weighing 250 g at the start of the protocols, obtained from the Instituto de Ciências Biológicas of the Universidade Federal de Minas Gerais. They were housed in polypropylene boxes (414 mm  $\times$  344 mm  $\times$  174 mm), with five animals per box, under a 12hour light-dark cycle, and provided with water and food ad libitum. The experimental procedures were evaluated and approved by the Animal Ethics Committee, under registration numbers 384/ 2018 and 116/2021.

Animals were divided into two protocols: 1) testing whether probing stimulation applied to the ipsilateral amygdaloid complex would affect propagation—Probing protocol; and 2) whether distinct temporal patterns of electrical stimulation applied to the contralateral amygdaloid complex could disrupt the propagation pattern—Propagation protocol.

The Probing protocol was designed with two groups: stimulation (n = 3) and control (n = 4). In both groups, seizures were induced with KA, but stimulation was applied only in the stimulation group. The Propagation protocol also included two groups: PS (n = 5) and NPS (n = 5). Again, seizures were induced with KA in both groups, but different stimulation patterns were applied.

#### **KA** Injection

In both protocols (Probing and Propagation), a guide cannula, made from a 22-gauge needle, was placed 1 mm above the CA3 region of the right ventral hippocampus for the Probing protocol -ipsilateral to stimulation electrode (coordinates relative to the bregma: -5.6 mm AP-antero/posterior, 4.3 mm ML-medial/lateral, and -5.5 mm DV-dorsal/ventral)—and the left ventral hippocampus for the Propagation protocol—contralateral to stimulation electrode (coordinates relative to the bregma: -5.6 mm AP, -4.3 mm ML, and -5.5 mm DV). This guide-cannula was later used to guide an injection cannula (exactly 1 mm longer than the guide cannula) for KA injection (2 mg/ML—18.8 mm KA—injected at a rate of 100 nl/min and a total volume of 200 nl) to produce a focal model of temporal lobe epilepsy.

# Stereotaxic Placement of Recording and Stimulation **Electrodes**

The animals from both protocols underwent stereotaxic surgery for the implantation of electrodes and the guide cannula. For the procedure, the rats were anesthetized with isoflurane (1 mL/mL, Isoforine®, Cristália Prod. Quím. Farm. Ltd) through an inhalation system with an induction rate set at 500 mL/min at 5% isoflurane. and maintenance between 100 and 200 mL/min at 2% to 3% isoflurane. The animals received local anesthesia with a 2% lidocaine hydrochloride and epinephrine solution and were positioned in the stereotaxic system (Stoelting Co, Wood Dale, IL). At the end of the surgery, the animals received a subcutaneous injection of the opioid antiinflammatory tramadol (3 mg/kg, diluted to a volume of 1 mL total) and a single dose of veterinary pentabiotics (Zoetis®). They were then rested and monitored for ≥five days until fully recovered.

The recording electrodes used in this work were developed manually using either tungsten microwires 99.5% S-Formvar with 50 μm internal diameter (California Fine Wire Co®, Grover Beach, CA -Probing protocol) or Teflon-coated stainless steel wire (Model: 791400, A-M Systems®, Carlsborg, WA - Propagation protocol). The

Teflon-coated stainless steel wires were intertwined, producing a twisted pair with a 0.5-mm distance between the exposed tips. This configuration also was used for the stimulating electrode pair. The number of recorded areas varied within each protocol because the Probing protocol aims to determine whether an ipsilateral stimulus interferes with seizure initiation and propagation (ie, to evaluate whether the probing stimuli may be used for seizure prediction as described in the literature). In contrast, the Propagation protocol aims to determine whether contralateral stimulation may attenuate seizure propagation to the contralateral hemisphere from the initial ictogenic foci.

The electrode headstage was assembled as detailed elsewhere 61 using a fiberglass board with drilled stereotaxic coordinates where the electrodes are aligned and fixed in position to accelerate surgery for multisite electrode placement. Each protocol had its own set of electrode implants: 1) The probing protocol had an arrangement of tungsten electrodes with bilateral hippocampal CA3 implants (AP -5.3 mm, ML ±4.3 mm, DV -6.0 mm; four electrodes per area separated by 100 µm each) and bilateral basolateral amygdala implants (AP -2.52 mm, ML ±4.8 mm, DV -8.8 mm; four electrodes per area separated by 100 µm each). The total number of recorded channels was 16. The stimulus electrode was placed in the right baso-lateral amygdala (AP -2,52 mm, ML -4,8 mm, DV -8.3 mm; twisted pair), ipsilateral to the KA injections site; 2) the Propagation protocol had an arrangement with two bilateral hippocampal implants—dorsal CA1 (AP -2.70 mm, ML ±2.0 mm, DV -2.6 mm; a twisted pair recording electrodes) and ventral CA3 (AP -5.6 mm, ML  $\pm 4.3$  mm, DV -7.2 mm; a twisted pair recording electrodes) and bilateral baso-lateral amygdala implants (AP -2.52 mm, ML ±4.8 mm, DV -8.8 mm; a twisted pair recording electrodes). The total number of recorded channels was 12, but only the better of each pair was used. The stimulus electrode was placed in the right baso-lateral amygdala (AP -2.52 mm, ML -4.8 mm, DV -8.3 mm; twisted pair 0.5 mm apart), contralateral to the KA injection site. Figure 1b shows the recording sites.

# Intraencephalic Local Field Potential Recordings and **Amygdaloid DBS**

The recordings were conducted using the headstage built with the Intan RHD2000 chipset and a surface mount device/flexible printed circuit female connector for both protocols: 16 channels for the Probing protocol and 12 channels for the Propagation protocol. The sampling rate was set at 10 kHz (16 bits successiveapproximation analog-to-digital converter), and an event channel was added to provide a synchronization signal between recording and stimulation.

Stimulation in the amygdala was a 100-µs pulse of 500 µA (DIGI-TIMER® Model: DS2A-Mk) at programmed interpulse intervals depending on the protocol. Both groups stimulated the amygdaloid complex; Probing stimulated the ipsilateral amygdala to determine whether it interferes with seizure initiation and propagation (ie, to evaluate whether the probing stimuli may be used for seizure prediction as described in the literature). In contrast, the Propagation protocol stimulated the contralateral amygdaloid complex (AMY) to assess whether contralateral stimulation may attenuate seizure propagation to the contralateral hemisphere from the initial ictogenic foci. The pulse was triggered by a transistor-transistor-logic output of an Atmel SAM3X8E ARM microprocessor Cortex-M3, programmed on the ARDUINO DUE platform. The pattern of stimulation used in the Probing protocol was set at a fixed 2-second interpulse

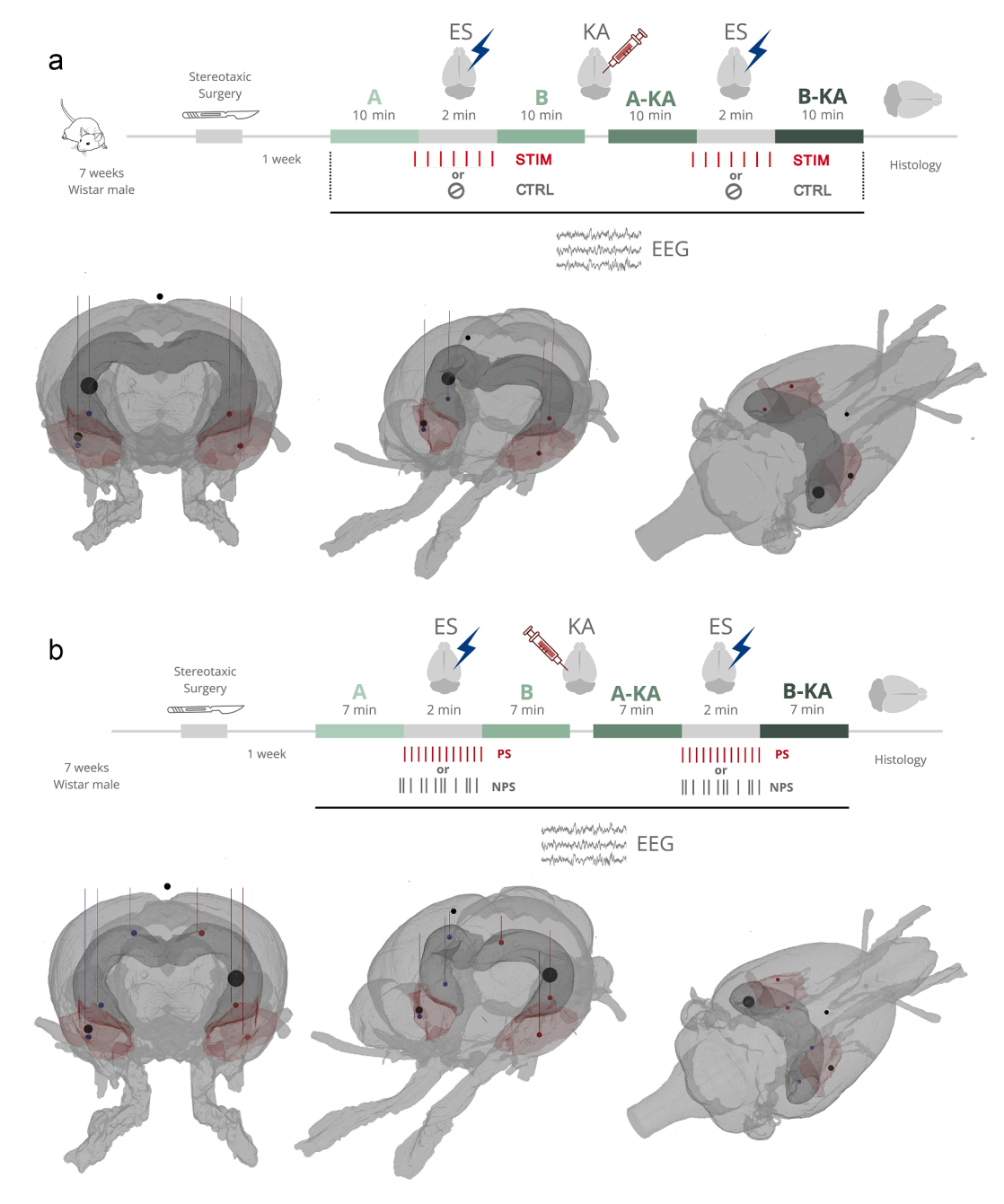


**Figure 1.** Design of the experimental protocols. a. Probing protocol. Experiment timeline (upper row), and diagram showing electrode placements and the positions of KA injections (bottom). b. Propagation protocol. Experiment timeline (upper row), and diagram showing electrode placements and the positions of KA injections (bottom). EEG, electroencephalogram. [Color figure can be viewed at <a href="https://www.neuromodulationjournal.org">www.neuromodulationjournal.org</a>]

interval (IPI = 2000 ms—0.5 Hz or no-stimuli group). The Propagation stimulation pattern was either a PS of 4 Hz (PS—250 ms IPI); or an NPS of four pulses per second on average (NPS with IPIs obeying an inverse decay histogram-power law distribution). The stimulation parameters were chosen on the basis of previous results regarding PS and NPS patterns. The NPS stimulus is a randomized but restrictive stimulation, whereas the PS is a regular and constant stimulation; however, both forms present a total of four stimuli per second, modifying only the temporal pattern governing the IPIs. These patterns were taken from a previous study showing proconvulsive properties for PS and anticonvulsant for NPS. Examples

of ARDUINO routines written in C++ for both the PS and NPS standards can be accessed at a GITHUB (https://github.com/nnc-ufmg/stimulator\_triggers). Figure 1 shows the stimulation patterns.

# **Electrophysiologic Statistical Analysis of Data**

Given the differences between the two data sets, preprocessing was conducted separately for each Protocol while adhering to a consistent set of procedures. The differences are minor and do not interfere with the hypothesis being tested in each protocol.

For the Probing protocol, the data were standardized to a 20-minute window, spanning 10 minutes before the first stimulus

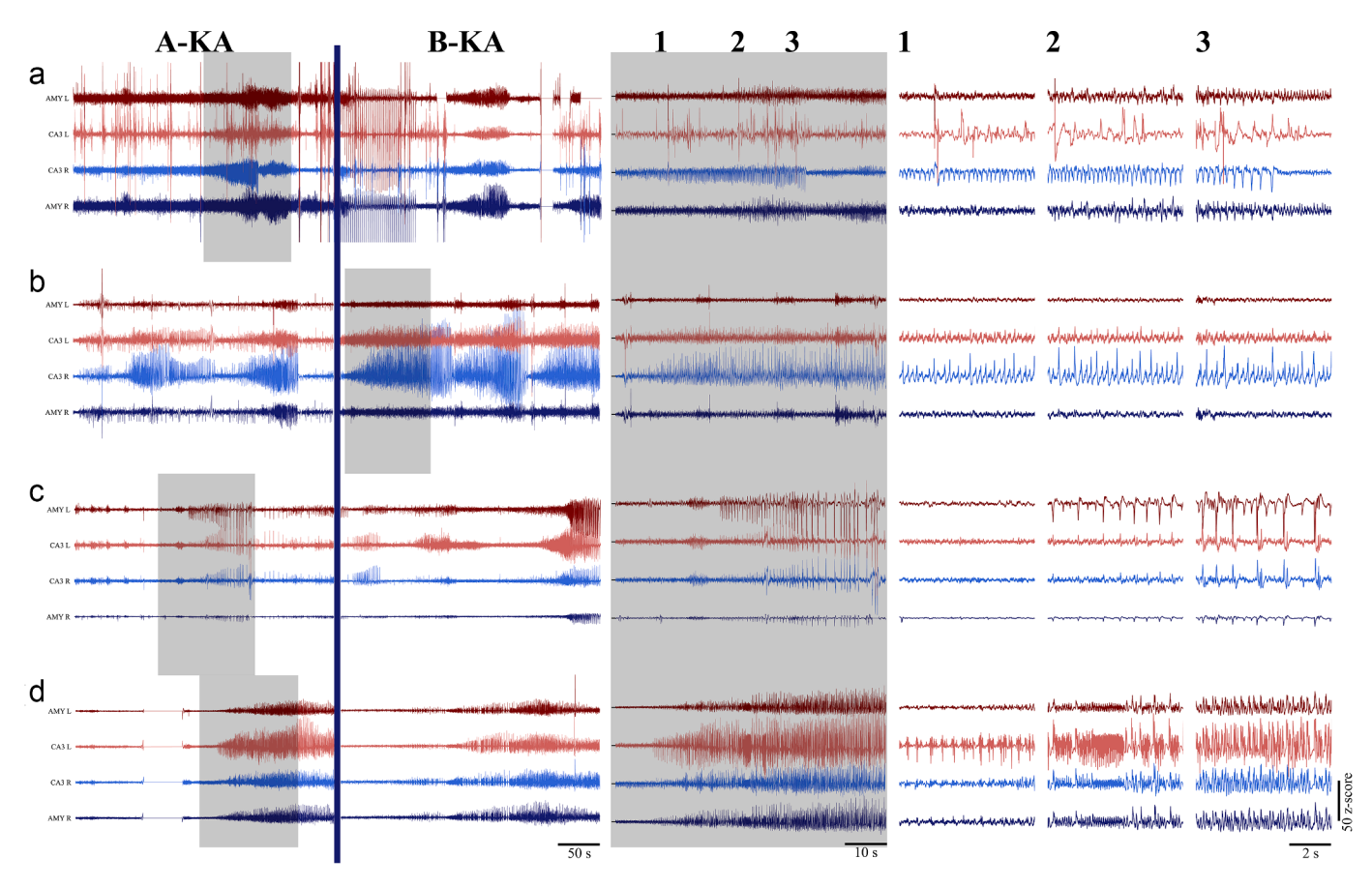


Figure 2. Examples of preprocessed electrophysiologic recordings extracted from control and stimulation groups, in which the left panel shows the different experiment sections, middle panel shows the gray highlighted area magnified, and the right panel shows the portions 1, 2, and 3 in detail. a. Segment of an animal of the stimulation group showing seizure starting in the ipsilateral hemisphere. b. Segment of an animal of the control group evidencing a seizure starting in the ipsilateral hemisphere with no propagation to the contralateral portion. c. Segment of an animal of the control group showing a seizure starting in the contralateral hemisphere with a subsequent propagation to the ipsilateral portion. d. Segment of an animal of the stimulation group evidencing a generalized seizure, at the end of the recording session. [Color figure can be viewed at www.neuromodulationjournal.org]

and 10 minutes after the last stimulus. Preprocessing steps included notch filtering at 60 and 120 Hz, bandpass filtering between 1 and 450 Hz, and resampling to 1000 Hz. The propagation protocol had a minor power line noise, requiring an additional harmonic (180 Hz) to be removed in the data from this protocol. This preprocessing step was not needed in the Probing protocol.

For the Propagation protocol, the data were standardized to a 14-minute window, spanning 7 minutes before the first stimulus and 7 minutes after the last stimulus. Preprocessing steps included notch filtering at 60, 120, and 180 Hz, bandpass filtering between 1 and 300 Hz, and resampling to 1000 Hz.

For both protocols, a graphical interface was constructed using the programming language Python combining the matplotlib library to visualize and pan the EEG signal and Tkinter for the selection of both seizures and noise. The procedure was performed such that the researcher was able to pan the EEG data, and when noise or a seizure event was identified, he was able to mark the corresponding portion of the signal, generating a label with a start and end samples. These labels were then saved in a JSON format for every instance of noise in every channel in the whole data and were later used to set the affected samples to zero so as to not interfere with the rest of the analysis, and the preprocessed data were segmented into four distinct phases: (A) before KA

administration and stimulation, (B) before KA administration but after stimulation, (A-KA) after KA administration but before stimulation, and (B-KA) after KA administration and stimulation (Fig. 1a,

Initially, data from each animal were calculated by aggregating the contributions of all channels, using five attributes related to the recorded seizures: 1) total number of seizures; 2) total duration of events; 3) total energy of events; 4) average seizure duration; and 5) average energy. After defining each attribute, the control and stimulation or PS and NPS groups were compared in two experimental stages: a) A-KA and b) B-KA. To compare the resulting distributions, the Wilcoxon rank-sum test for two samples was applied, followed by a false discovery rate (FDR) correction using the Benjamini-Hochberg procedure. Attributes 1), 2), and 3) were corrected together, given they relate to seizure occurrence, whereas 4) and 5) were corrected together because they reflect seizure severity. Moreover, effect sizes were calculated using the rank-biserial correlation. Only the relevant results are shown in Figure 2a and Figure 5a, and a left-tailed rank-sum test was used for the intergroup analysis involving discrete countable data using a significance level of 0.05.

In the second step, using the same five attributes, the data were analyzed at the channel level. Again, analyses were conducted separately for the two experimental stages: a) A-KA and b) B-KA,

<b>Table 1.</b> Contingency Table Showing the Relation Between Preceding Channel X and Subsequent Y.					
		Y hap	Y happening after or at the same time as X		
		Ch Y	Ch ~Y	SUM row	
Channel X preceding channel Y	Ch X	а	b	a+b	
	Ch ~X	C	d	c+d	
	SUM col	a+c	b+d	a+b+c+d	
Ch, channel.					

with additional separation by left and right hemisphere. We used generalized linear models using Generalized Estimating Equations (GEE)—a Poisson model for count data and a Gaussian model for continuous data—to compare the control and stimulation (PS and NPS) groups. This approach accounts for the nonindependence of observations from the same subject given each animal contributes data from multiple recording channels. Although the models treated channels as repeated measures within animals, we opted to present the results by channel to improve clarity and to report them in the text using grouped medians and interquartile ranges. Results are presented in Figure 2b,c and Figure 5b,c, along with FDR-corrected *p*-values (Benjamini-Hochberg correction) and effect sizes (Cohen's *d* for continuous variables and rate ratios for Poisson models).

The univariant analysis previously conducted did not allow a proper evaluation of the sequential propagation of ictogenic events determined by interchannel relations. When evaluating functional connectivity, researchers often use techniques such as crosscorrelation, coherence, phase synchronization, or Granger causality. Each of these methods has its strengths in evaluating the temporal and directional relationships between brain signals. However, in our situation, the unique characteristics of our data—specifically, the discrete and small number of ictal-like electrographic activity episodes—meant we needed to take a different approach.

Traditional methods, such as Granger causality, typically work under the assumption of continuous time series data and are most effective for uncovering predictive relationships within signals. Given the discrete nature of our observations, we opted for a more suitable approach based on an analytical method commonly used in neuroethologic research (ie, quantifying the likelihood of behavioral association sequences). 62,63 A series of contingency tables are designed to determine whether the cooccurrence of events across various brain regions could be attributed to chance alone (probability close to 1) or some measure of propagation relation (probability close to 0). This strategy enabled us to draw meaningful conclusions about functional relationships in the context of seizure propagation while avoiding the assumptions inherent in continuous dynamics. It is noteworthy that, much like Granger causality, our method does not suggest mechanistic causality. Rather, it emphasizes probabilistic associations that are directly relevant to the specific questions we sought to answer in this study. Thus, a prior statistical assumption regarding the NULL hypothesis is that circuits do not have obvious and immediate generalized activity.

Therefore, a more detailed analysis of specific relationships between channels was conducted using a set of contingency tables for each seizure (Table 1), where the rows represent events related to a recorded channel (channel X), and the columns represent events related to another selected channel (channel Y).

The Boschloo test (derived from the Fisher exact test) was used to assess the probability that a particular sequence between two channels occurred by chance, whether unlikely or very likely. This was accomplished using relational contingency tables to create a  $6 \times 6$  matrix (Fig. 2d and Fig. 5d) of channel sequential recruitment, as later described.

Using the Propagation protocol as an example, channels X and Y represent any of the six channels recorded, CA1R, CA1L, CA3R, CA3L and AMYR, AMYL (completely analogous for the Probing protocol set of channels, where R and L stand for right and left, respectively). The terms in the table represent a) the number of times Y happened after or at the same time as X; c) the number of times Y happened after or at the same time of any other channel other than X; b) the number of times any other channel than Y happened after or at the same time as X; and d) the number of times any other channel than Y happened after or at the same time as any other channel but X. Therefore, the terms (a+c) refer to the number of times Y happened after or at the same time as any channel; (b+d) any channel aside from Y happening after or at the same time as any other channel; (a+b) X preceding (or at the same time) as any other channel; and (c+d) any channel other than X preceding (or at the same time) as any other channel. The p-values retrieved from the tables as previously described indicate the probability that the relationship between X and an ictal event in Y, occurring either before or simultaneously, could arise by chance on the basis of the ratios presented. Therefore, p-values close to 1 suggest no relationship between X and Y, whereas p-values near 0 indicate strong evidence that these channels are connected in their activity patterns. It is important to note that the  $6 \times 6$  matrix, displaying all possible combinations, is not symmetric, given the table for X-Y may differ from that for Y-X. Moreover, the diagonal column was excluded given X-X combinations do not contribute to channel correlations. Thus, for each seizure, 30 contingency tables were generated, representing all possible channel combinations except those involving the same channel. The tables obtained for each seizure were then compiled as a single table within each group, generating 30 contingency tables for the PS group and another 30 for the NPS

To assess the probability of directed seizure propagation between pairs of brain regions, we used Boschloo's test—a more powerful variant of Fisher exact test—on  $2 \times 2$  contingency tables summarizing the temporal order of ictal events. This method is particularly well suited for our data, which comprise sparse, discrete events, and offers greater statistical power while maintaining control over type I error rates. Each resulting table was statistically analyzed, and the corresponding p-values are represented by the matrices in Figures 2d and 5d, where the rows indicate the predecessor channels relative to seizure onset, and the columns indicate the successor channels.

#### **Histologic Procedures**

At the end of the recordings, the animals were anesthetized with an intraperitoneal solution of ketamine (80 mg/kg) and xylazine (30 mg/kg). The position of the electrodes was confirmed by an electrolytic lesion (0.5 mA for 2 seconds), and the animals were then subjected to a cardiac perfusion protocol with phosphatebuffered saline solution (PBS) 0.1 M (0.387 M NaH2PO4.H2O; 0.612 M Na2HPO4.7H2O; 1.4 M NaCl) pH = 7.4, followed by a solution of paraformaldehyde (PFA) dissolved in PBS (PFA/PBS; 4% w/v; pH = 7.4). The brains were then removed, postfixed in PFA/PBS 4% weight in volume (w/v), and kept at 4 °C for 24 hours. The brains were subsequently sectioned (40 µm) using a cryostat (Leica®), and some slices, on the basis of stereotaxic coordinates related to the implantation sites of the recording electrodes and the cannula, were selected and stained to confirm the implantation sites, following a marking protocol with neutral red solution (neutral red 1% w/v; anhydrous sodium acetate 0.3% w/v; glacial acetic acid 0.12% volume/volume).

# **RESULTS**

# **Probing Protocol**

Figure 3a,b,c,d, along with the zoomed-in insets, illustrates the quality of the electrophysiologic recordings from both stimulation and control groups. The gray boxes and dashed lines indicate the intervals in which the electroencephalogram was depicted in the insets. The examples were chosen to represent situations in which electrographic seizure-like activity started at different locations for both stimulation and control regarding laterality in terms of the KA injection site.

The results obtained indicate that there were no significant differences when analyzing the seizure events across groups that received (stimulation) and did not receive (control) the 0.5-Hz stimulation (total seizures A-KA-CONTROL: 4 [2.5-4.5], STIMULA-TION: 2.5 [2-3], p = 0.760, e.s. = 0.331; mean duration A-KA-CONTROL: 67.719 [67.439-92.373], STIMULATION: 62.678 [54.543-139.545], p = 0.638, e.s. = -0.233; mean energy A-KA-CONTROL: 95.341 [93.368-95.948], STIMULATION: 16.730 [5.649--30.942], p = 0.983, e.s. = 0.946; total seizures B-KA-CONTROL: 4 [4–5.5], STIMULATION: 2 [1.5–2], p = 0.975, e.s. = 0.845; mean duration B-KA-CONTROL: 57.167 [54.175-60.313], STIMULATION: 42.665 [42.204–114.442], p = 0.744, e.s. = -0.324; mean energy B-KA-CONTROL: 73.218 [61.094-79.803], STIMULATION: 33.022 [27.412-64.446], p = 0.744, e.s. = 0.354. All statistical tests in this section were performed using the Wilcoxon rank-sum test), thus showing that it did not have a significant effect on the seizure events, when comparing combined data across total seizures, interhemispheric seizures, total and mean seizure duration, and total and mean energy. The trend in these findings continues in the analysis considering only the separate sections, A-KA and B-KA, in which the p-values remain not significant.

Regarding the number of seizure events per channel, the results show that there were no significant differences when analyzing the seizure events across the channels, when comparing combined data across total seizures, total and mean seizure duration, and total and mean energy (total seizures A-KA-CONTROL: 2 [1–3], STIMULATION: 2 [2–2], p=0.807, e.s. =0.941, GEE Poisson; total duration A-KA-CONTROL: 50.794 [37.101–69.050], STIMULATION: 55.399 [48.868–197.875], p=0.349, e.s. =-2.279, GEE Gaussian; total energy A-KA-CONTROL: 21.612 [11.465–80.935], STIMULATION: 6.272 [1.596–10.606], p=0.053, e.s. =1.221, GEE Gaussian; mean duration A-KA-CONTROL: 67.159 [53.107–67.159], STIMULATION: 51.489 [48.304–260.851], p=0.268,

e.s. = -1.620, GEE Gaussian; total duration B-KA-CONTROL: 27.748 [12.236-63.499], STIMULATION: 46.630 [42.665-48.249], p = 0.177, e.s. = 0.937, GEE Gaussian; total energy B-KA-CONTROL: 15.222 [10.641–42.158], STIMULATION: 10.966 [4.506–30.220], p = 0.053, e.s. = 1.739, GEE Gaussian; mean duration B-KA-CONTROL: 42.375 [32.439–45.475], STIMULATION: 42.665 [42.665–73.175], p = 0.268, e.s. = -1.839, GEE Gaussian; mean energy B-KA-CONTROL: 25.779 [12.306-29.476], STIMULATION: 10.343 [4.794-29.574], p = 0.268, e.s. = 1.063, GEE Gaussian). However, the mean energy in the A-KA section and total seizures in the B-KA section scored a p-value of < 0.001 (mean energy A-KA-CONTROL: 29.567 [18.892-54.954], STIMULATION: 9.348 [1.795–10.523], \*p = < 0.001, e.s. = 2.149, GEE Gaussian; total seizures B-KA-CONTROL: 4 [2–5], STIMULATION: 1 [1–2], \*+p = <0.001, e.s. = 0.327, GEE Poisson), suggesting a significant difference when comparing the different channels in the control and stimulation groups. Finally, when analyzing seizure events per electrode, there were no significant differences in seizure events metrics across right and left electrodes in the A-KA and B-KA sections (total seizures A-KA (right)-CONTROL: 1 [1-3], STIMULATION: 2 [2-2], p = 0.944, e.s. = 0.909, GEE Poisson; total duration A-KA (right)–CONTROL: 64.400 [43.877–70.941], STIMULATION: 54.415 [47.703–164.003], p = 0.606, e.s. = -1.711, GEE Gaussian; total energy A-KA (right)-CONTROL: 33.573 [13.373–85.632], STIMULATION: 5.409 [1.584–11.063], p = 0.378, e.s. = 0.940, GEE Gaussian; mean duration A-KA (right)-CONTROL: 67.159 [53.107-67.159], STIMULATION: 51.489 [49.574-162.525], p = 0.327, e.s. = -6.690, GEE Gaussian; mean energy A-KA (right)-CONTROL: 29.567 [19.409-58.165], STIMULATION: 10.343 [1.795–12.022], p = 0.066, e.s. = 1.530, GEE Gaussian; total seizures A-KA (left)-CONTROL: 2.500 [1.750-3.000], STIMULATION: 2.000 [2.000–2.250], p = 1.000, e.s. = 1.000, GEE Poisson; total duration A-KA (left)-CONTROL: 47.284 [35.385-67.159], STIMULATION: 55.399 [51.381–197.875], p = 0.378, e.s. = -3.147, GEE Gaussian; total energy A-KA (left)-CONTROL: 14.192 [8.823-23.592], STIMULATION: 6.272 [2.339–9.379], p = 0.378, e.s. = 13.345, GEE Gaussian; mean duration A-KA (left)-CONTROL: 64.563 [55.607-69.970], STIMULATION: 151.025 [48.448-257.122], p = 0.205, e.s. = -1.638, GEE Gaussian; mean energyA-KA (left)-CONTROL: 31.259 [16.375-46.458], STIMULATION: 6.854 [3.548-9.616], p = 0.066, e.s. = 2.039, GEE Gaussian).

The analysis of functional connectivity during seizure events revealed a lack of predictability in the analyzed brain regions, regardless of the experimental condition (Fig. 2d). In both the control and stimulation groups, seizures were detected simultaneously across channels, with *p*-values predominantly equal to 1.0, indicating no temporal delay between regions. This suggests that seizure activity occurred synchronously across the evaluated network, making it difficult to identify directional propagation patterns.

Although some p-values were lower in the B-KA section, particularly in connections such as CA3R–CA3L and CA3L–AMYL in the control group, and CA3R–CA3L in the stimulation group, these differences did not reach statistical significance ( $p \geq 0.05$ ), reinforcing the absence of systematic delays among channels (Fig. 1). The lack of significant connectivity differences suggests that seizure activity does not follow a predictable propagation pattern within the analyzed structures

# **Propagation Protocol**

Figure 4a,b,c,d, along with the zoomed-in insets, illustrates representative examples of electrophysiologic recordings from both the PS and NPS groups during the Propagation protocol. In the PS group, generalized seizures were selected, with one initiating in the left hemisphere (Fig. 4a) and another in the right hemisphere (Fig. 4b). In

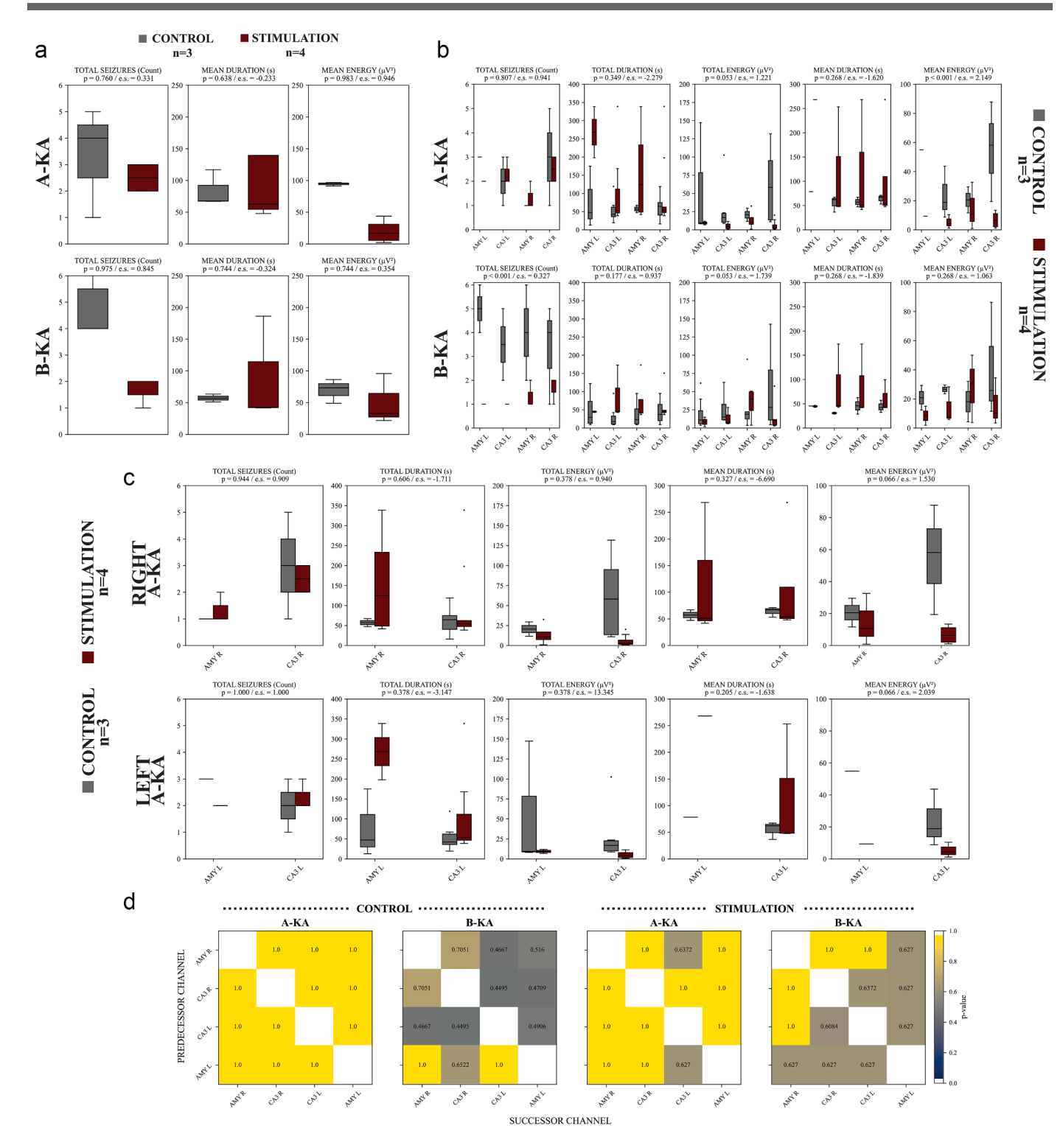


**Figure 3.** a. Seizure metrics comparison between control and stimulation groups across all data during A-KA and B-KA sections. b. Analyses of seizure events per channel using GEE models, showing a significant difference in mean energy in the A-KA section (p < 0.001) and total seizures in the B-KA section (p < 0.001). c. No significant difference in seizure events per electrode for A-KA and B-KA when analyzed using GEE models. Panel d shows the statistical analysis of seizure causality between brain regions in control and stimulation groups under A-KA and B-KA protocols. p = 1.0 (shaded from yellow to dark blue) indicates simultaneous seizure detection across channels, whereas lower p-values suggest temporal offsets. [Color figure can be viewed at <a href="https://www.neuromodulationjournal.org">www.neuromodulationjournal.org</a>]

contrast, the NPS group shows distinct episodes: one restricted to the left hemisphere (Fig. 4c) and another that generalized bilaterally but remained confined to the hippocampus with low amplitude (Fig. 4d).

The analysis of seizure occurrence per animal revealed no significant difference between groups (total seizures A-KA-NPS: 0 [0–1] PS: 2 [1–2], p = 0.087, e.s. = 0.429, Wilcoxon rank-sum test

3

1

3

2

synchronized activity across areas at the onset of a generalized seizure that recruits all channels. b. Segment from an animal in the PS group showing a generalized seizure that clearly affects the right hemisphere more than the left hemisphere at the beginning of the seizure. c. Segment from an animal in the NPS group showing a hippocampal focal seizure. d. Segment from an animal in the NPS group showing a low-amplitude seizure recorded in both hippocampi. [Color figure can be viewed at www.neuromodulationjournal.org]

and total seizures B-KA-NPS: 0 [0-2] PS: 1 [1-2], p = 0.202, e.s. = 0.264, Wilcoxon rank-sum test). However, statistical comparisons identified group differences in mean seizure energy (mean energy B-KA-NPS: 0 [0-2.023] PS: 11.962 [5.094-36.646], \*p = 0.047, e.s. = 0.627, Wilcoxon rank-sum test) and a trend toward significance in mean seizure duration during the B-KA period (mean duration B-KA-NPS: 0 [0-22.595] PS: 43.492 [22.292–95.419], p = 0.087, e.s. = 0.429, Wilcoxon rank-sum test)—

A-KA

а

**B-KA** 

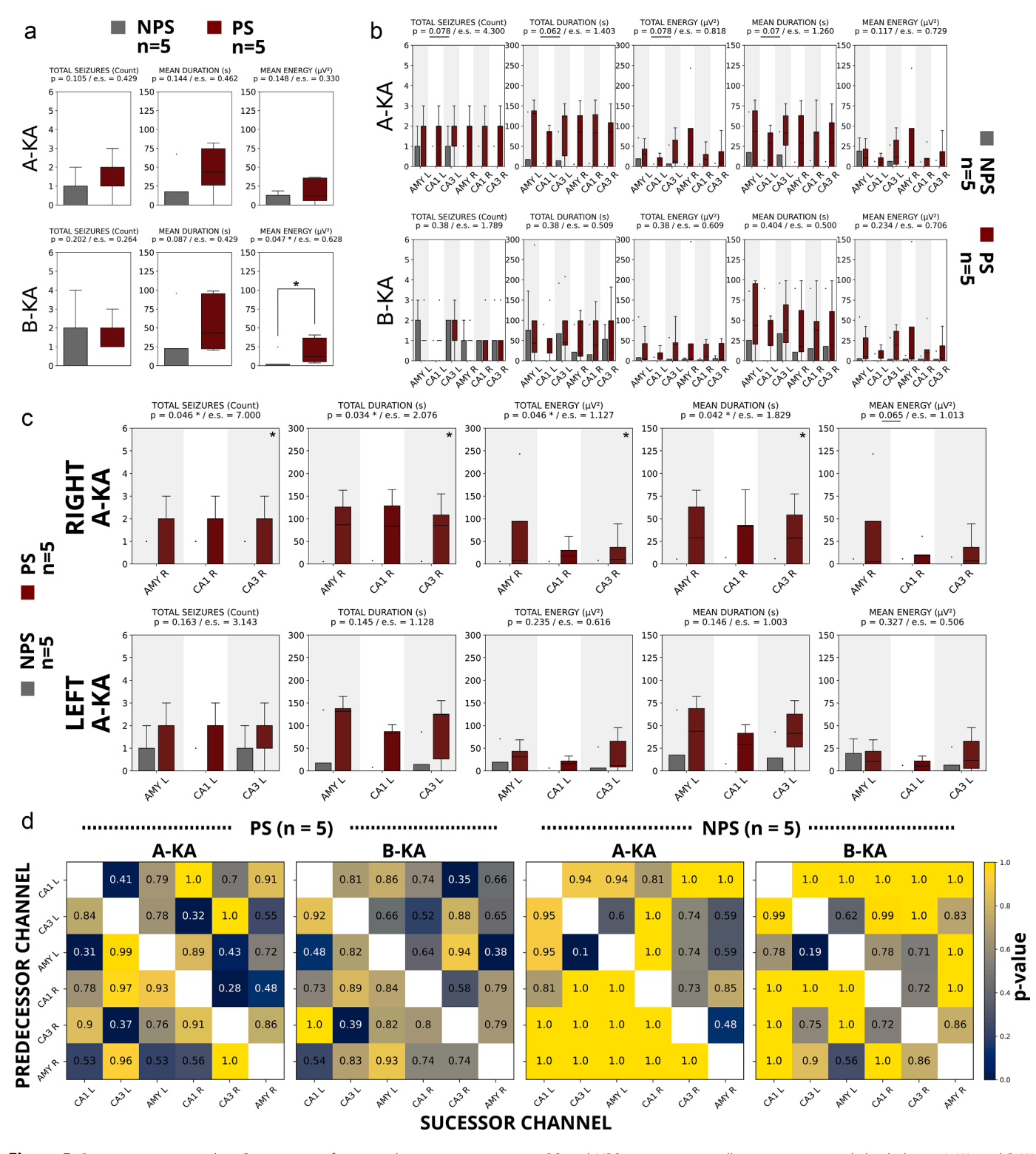


**Figure 5.** Propagation protocol. a. Comparison of extracted seizure parameters in PS and NPS groups across all seizure events, subdivided into A-KA and B-KA periods. b. Overall effect comparison using GEE, revealing significant differences between PS and NPS across most parameters during the A-KA period. c. GEE-based comparison of stimulation effects during the A-KA period, further subdivided by hemisphere. d. Seizure causality analysis between brain regions in PS and NPS groups during both A-KA and B-KA periods. Shading from yellow to dark blue indicates increasing interregional sequential relationships, as described in the section titled Electrophysiologic Statistical Analysis of Data. [Color figure can be viewed at <a href="https://www.neuromodulationjournal.org">www.neuromodulationjournal.org</a>]

both indicative of seizure severity once triggered. The limited number of seizures, which is typical in short-term chemically induced models, likely contributed to the absence of statistical significance for some parameters in Figure 5a. Nevertheless, these findings suggest a more severe ictal state in the PS group during the later stages of the protocol. Figure 5b reveals a distinct

modulatory effect of the stimulation pattern, with borderline differences (p < 0.05 or trending, with large effect sizes) across all parameters during the A-KA period, as determined by global comparisons using the GEE model (total seizures A-KA NPS: 0 [0–0.75] PS: 2 [0–2], p = 0.078, e.s. = 4.3, GEE Poisson; total duration A-KA NPS: 0 [0–4.086] PS: 86.132 [0–127.816], p = 0.063, e.s. = 1.4, GEE Gaussian; total energy A-KA NPS: 0 [0–4.23] PS: 13.856 [0–41.611], p = 0.078, e.s. = 0.818, GEE Gaussian; mean duration A-KA NPS: 0 [0–4.086] PS: 35.205 [0–60.55], p = 0.07, e.s. = 1.26, GEE Gaussian; mean energy A-KA NPS: 0 [0–4.23] PS: 7.274 [0–20.806], p = 0.117, e.s. = 0.729, GEE Gaussian).

In summary, these results suggest a potential propagation-interference effect of NPS compared with PS through two complementary mechanisms: Figure 5b indicates early modulation (A-KA). In contrast, Figure 5a suggests a delayed effect (B-KA). Notably, both protocols delivered the same number of stimuli to the same brain region (AMYR), differing only in their temporal organization.

The differential effect of PS vs NPS in preventing seizure propagation to the right hemisphere is more clearly illustrated in Figure 5c. NPS showed superior efficacy during the A-KA period, particularly in the right hemisphere (upper panels), corresponding to the stimulation site (total seizures A-KA NPS: 0 [0–0] PS: 2 [0–2], \*p = 0.046, e.s. = 7, GEE Poisson; total duration A-KA NPS: 0 [0-0] PS: 85.697 [0-127.185], \*p = 0.034, e.s. = 2.076, GEE Gaussian; total energy A-KA NPS: 0 [0-0] PS: 10.318 [0-48.996], \*p = 0.046, e.s. = 1.127, GEE Gaussian; mean duration A-KA NPS: 0 [0-0] PS: 28.856 [0-58.57], \*p = 0.046, e.s. = 1.829, GEE Gaussian; mean energy A-KA NPS: 0 [0–0] PS: 3.439 [0–24.498], p = 0.065, e.s. = 1.013, GEE Gaussian). Although no statistically significant differences were observed in the contralateral (left) hemisphere, several parameters approached significance (total seizures A-KA NPS: 0 [0–1] PS: 2 [0–2], p = 0.163, e.s. = 3.143, GEE Poisson; total duration A-KA NPS: 0 [0-11.057] PS: 86.772 [0–128.352], p = 0.145, e.s. = 1.128, GEE Gaussian; mean duration A-KA NPS: 0 [0-11.057] PS: 41.485 [0-56.823], p = 0.146, e.s. = 1.003, GEE Gaussian). Nevertheless, they showed large effect sizes, suggesting a possible anticonvulsant effect of NPS in focally induced KA seizures even when stimulation occurs in the contralateral hemisphere.

A more targeted investigation of interchannel relationships was conducted using the contingency table approach described in the section titled Electrophysiologic Statistical Analysis of Data. Figure 5d shows that NPS reduces the likelihood of left-to-right probability of sequential activation compared with PS during both the A-KA and B-KA periods, as indicated by darker matrix cells (representing stronger interchannel sequential relationships). Notably, a consistent interaction between AMYL and CA3L was observed in the NPS group across both periods. Although not statistically significant, the low *p*-values suggest that this effect is unlikely to have occurred by chance.

# DISCUSSION

In this work, we aimed to study 1) whether a probing stimulation applied to the ipsilateral amygdaloid complex (ie, for seizure prediction) would affect propagation, 2) the propagation pattern of epileptiform activity due to focal intrahippocampal injections of KA during the status epilepticus, and 3) whether distinct temporal patterns of electrical stimulation applied to the contralateral amygdaloid complex could interfere with the ictogenic propagation pattern. The NPS aimed to restore homeostasis in a focal

epilepsy animal model, even at the cost of increasing excitation, when circuit competition is knowingly compromised. The imbalance caused by the ictogenesis process, induced by intrahippocampal KA injection, 62,63 fosters a "winner-takes-all" (WTA) dynamic, 64 favoring a single attractor (or a reduced number of attractors restricted to specific circuits) and eventually destabilizing the entire network. Circuit disorganization before seizure activity has been observed as low-voltage fast activity (LVFA, >14-100 Hz<sup>65-68</sup>), provoked by the hyperactivation of inhibitory interneurons. This apparent paradox can be explained by competitive microcircuits that aggregate and synchronize to form a "winner circuit motif" during the ictogenesis process. In this context, the role of inhibitory interneurons makes sense only if their functional aspect is more closely related to sharpening the coincidence detection circuit framework than to the classical view of excitation-inhibition imbalance. This interpretation aligns with the view that LVFA is not merely a desynchronizing biomarker but rather an emergent property of competitive microcircuits during ictogenesis. In this sense, LVFA reflects the network-wide dynamics that precede the selection of a dominant circuit motif, consistent with a WTA process. Although the WTA selection may remain subthreshold, the electrographic expression of LVFA provides a detectable signature of this competition. Thus, instead of representing a paradox, LVFA can be viewed as a mechanistic feature of ictogenesis. Although this interpretation is supported by the consistency of the electrographic pattern across seizures, we acknowledge that the WTA model remains a hypothesis. 64,69 In any case, our results indicate that NPS disrupted the abnormal hyperconnectivity pattern to the contralateral hemisphere (Fig. 5), interfering with the seizure propagation pattern. Interestingly, the neuromodulatory effect of NPS before chemically induced seizures made the ictogenic process less likely to propagate contralaterally, whereas PS facilitated the recruitment of the contralateral hemisphere. These data support a significant argument for the viability of open-loop therapy with NPS, especially considering previously published findings with both NPS and probing stimuli, as elaborated in the later paragraphs.

Moreover, this work revealed that the number of seizures was not significantly affected by ipsilateral probing stimulation, which is recognized as effective in predicting seizure onset. 10,51,70-73 However, there were minor variations in seizure duration during ictogenesis (Fig. 2b), suggesting that the probing signal may not be as innocuous as previously suggested and therefore should be cautiously applied. Nonetheless, the observed effect did not seem to facilitate the process of triggering seizures but rather to amplify ictal electrographic activity once it had begun. In any case, one should always consider adjusting parameters of the probing stimulus to exclude any undesired effect while still yielding signals that allow seizure detection or prediction, such as further decreasing amplitude and firing rate. In summary, our results, along with previously published data from our laboratory, corroborate the proposal of a closed-loop solution involving the Probing protocol for seizure detection and the Propagation protocol for seizure attenuation. 10,11,74 It is important to highlight that the experimental procedure and data presented in this work focus on the seizure propagation effects of stimuli when applied to a focal animal model of seizure (ie, KA injection). However, the overall application of temporally coded stimulation for seizure prediction and attenuation, in addition to its use in a closed-loop system, is better substantiated by considering previously published data from our group.

Our findings contribute to the existing literature, showing that DBS application to modulate ictogenesis and epileptogenesis has yielded promising results in epilepsy treatment by altering the neural circuits involved in seizure generation and propagation, as can be observed in the review.<sup>22</sup> Although modern DBS protocols are primarily established for movement disorders, 75,76 there is a growing body of research supporting its application in psychiatric conditions such as depression and obsessive-compulsive disorder. 77,78 Recent studies have highlighted the need to adapt stimulation parameters for these indications rather than reusing protocols originally developed for motor symptoms.<sup>23,53</sup> Early mechanistic hypotheses proposed that high- or low-frequency DBS would activate or suppress neural networks, restoring function or inhibiting dysfunction.<sup>12,79</sup> Building on these insights, this research, along with other temporally coded DBS strategies found in the literature, operates under a distinct framework based on the hypothesis that stimulation may disrupt or facilitate large-scale integration of information among brain regions by influencing synchronization and the temporal organization of the underlying neural networks. 22,49,80 Despite differences in specific methods, the shared goal across various DBS approaches remains consistent: creating competing circuits to restore network homeostasis and redirect the system away from instability while promoting balanced circuit dynamics.<sup>81</sup> For instance, Tass et al use a method known as "Coordinated Reset" to stimulate multiple sites with uncorrelated temporal stimulation patterns, generating disruptive spatiotemporal stimulation aimed at preventing synchronization and the propagation of epileptiform activity.  $^{17,82,83}$  Our group also used multisite stimulation patterns, 48,50,52 as previously described; nevertheless, we also showed that PS and NPS interfere with the ictogenesis process in various epilepsy animal models, even when applied to a specific site. 14,51,60,81 This work not only supports data indicating that PS facilitates propagation to the stimulated region and that NPS interferes with the propagation process but also advances the idea that both PS and NPS exert a priming effect when applied to the contralateral hippocampus, thus affecting seizure propagation even when used before seizure induction by KA. This finding is particularly relevant for neuromodulation through DBS using an open-loop framework (eg, DBS Medtronic Percept®) because it suggests that NPS might have a sustained anticonvulsant effect on the underlying neural network (indicated by our A-KA data for NPS in the Propagation protocol). However, our results do not preclude its use when paired with a predictive system for seizures, triggering NPS in a closed-loop configuration.

The observed effects of PS and NPS highlight a critical interplay between network dynamics and seizure propagation mechanisms. This interplay may be closely influenced by mechanisms similar to "priming," wherein stimulation patterns influence the recruitment and balance of neural circuits. Understanding this relationship provides a deeper context for ways specific DBS strategies can modulate ictogenesis by either disrupting or reinforcing circuit activity, ultimately shaping the evolution of seizures. The term "priming," borrowed from memory research, 84,85 describes a phenomenon whereby exposure to a stimulus influences the response to subsequent stimuli by facilitating the recruitment of preactivated neural pathways, thus making it easier to process or recall associated information. Our findings suggest that the nonperiodic stimulus applied to the contralateral ictogenic foci interferes with this propagation of information, most likely by exciting a diverse population of competing circuits; conversely, the periodic stimulus pattern would consistently activate the same circuitry,

providing it with an "edge" during the WTA ictogenesis process. Moreover, although previous studies have suggested that PS at 0.5 Hz shows promise for seizure prediction, 10,11 this parameter (although not potentiating seizure initiation) slightly affected the underlying network during the ictogenesis process (Fig. 3b—mean energy, total seizures). Unsurprisingly, if probing stimulation is useful for seizure prediction, it would be expected to trigger shortterm plastic changes in the underlying network that could influence seizure duration (Figs. 2 and 3). de Castro Medeiros et al<sup>10</sup> showed that by pairing probing stimulation with seizures, it was possible to induce plastic changes in the underlying network so that further seizures could be predicted from the evoked responses—the process was named a programmable surrogate marker. Thus, it is reasonable to assume that "some" plastic changes are necessary to have a properly working probing stimulation for seizure prediction, provided it does not trigger the initiation of seizures themselves.<sup>86</sup> The frequency of repetition of these constant IPI stimulations is quite relevant in differentiating the probing effect from the proconvulsant effect, that is, compared with the PS. In both cases, temporally fixed stimuli may facilitate same-circuit representations within hippocampal neural networks, whereas NPS may disrupt them. In this context, epilepsy may be interpreted as a brain state of facilitated entrainment effect on the neural network, suggesting that epileptogenesis is a process that shares many mechanistic steps with memory formation—a pathologic memory facilitating a circuit that hijacks the entire network. It would be interesting to investigate further the possible long-lasting effects of NPS in spontaneous-recurrent-seizure models of epilepsy.

Another interesting result was that in some cases, the contralateral site from foci induction began to exhibit epileptiform activity before any other area. This, of course, only occurred after ≥one episode of secondary contralateral recruitment occurred owing to propagation from the ipsilateral foci. Overall, our data indicate that even during the Probing protocol (and during the Propagation protocol), KA-induced status epilepticus evolves into short-term plastic changes, allowing a secondary focus to eventually take control of the system. Literature has reported the secondary recruitment of the contralateral hippocampus during KAinduced status epilepticus, 87 with population oscillations generated both ipsilaterally and contralaterally to KA injection but with marginal long-term effects on contralateral hippocampal circuitry reorganization. Still, the present work indicates that such a contralateral secondary focus can generate and sustain seizures independently of the primary focus. The argument against intrahippocampal KA as a "strictly focal" animal model does not negate the validity of the hypothesis being tested once NP interfered with contralateral recruitment and seizure propagation. Nonetheless, this observation would benefit from proper quantification and a larger number of animals within each group—particularly given this phenomenon was not evident in every instance of KA-induced status epilepticus. Moreover, although we observed evidence for the independent recruitment of epileptiform activity in the contralateral hippocampus, further studies should investigate whether the epileptogenic plastic changes also extend to the contralateral hippocampus after the latent period for spontaneous recurrent seizures.

In summary, our findings confirm that the propagation of seizures during KA status epilepticus is influenced by the time-coded stimulation pattern used, provided that the total number of stimuli and the stimulated area are the same, offering novel insights into the dynamics of ictogenesis and possibly epileptogenesis. In addition, probing stimulation did not potentiate seizure initiation but did influence the ictal process after initiation, showing that it was not entirely innocuous in the ictogenic process. Nevertheless, seizure prediction protocols using chemically induced models, such as ours, fall outside the scope of spontaneous seizure prediction, and this is arguably an appropriate context for evaluating predictive algorithms. However, our focus was on understanding the effects of stimulation on seizure propagation and evaluating its potential impact on ictogenesis and epileptogenesis.

#### CONCLUSION

Our results show no evidence that probing stimulation to the ipsilateral amygdaloid complex (focal seizure KA animal model) facilitates seizure induction or propagation. Temporally coded neuromodulation interfered with seizure propagation patterns even if applied before (or after) the KA induction of focal seizures. Altogether, our results support the feasibility of a closed-loop therapeutic approach for seizure control, combining probing stimulation for seizure prediction with temporally coded DBS to disrupt seizure propagation.

# **Authorship Statements**

Márcio Flávio Dutra Moraes undertook writing—original draft, validation, supervision, resources, project administration, funding acquisition, and conceptualization. Vinícius Rosa Cota undertook writing—review and editing, and validation. Matheus Costa Passos undertook writing—review and editing, visualization, software, formal analysis, and data curation. João Pedro Carvalho-Moreira undertook writing—review and editing, visualization, validation, software, investigation, formal analysis, and data curation. Leonardo de Oliveira Guarnieri undertook writing—review and editing, validation, supervision, methods, investigation, data curation, and conceptualization. Thiago Moreira Maia Montalvão undertook conceptualization, methods, investigation, and data curation. Larissa Samara Santos Xavier undertook conceptualization, methods, investigation, and data curation.

# Conflict of Interest

The authors reported no conflict of interest.

# How to Cite This Article

Santos Xavier L.S., Maia Montalvão T.M., de Oliveira Guarnieri L., Carvalho-Moreira J.P., Passos M.C., Cota V.R., Moraes M.F.D. 2025. Distinct Patterns of Temporally Coded Electrical Stimulation Interfere With Long-Range Interhemispheric Coupling in a Focal Model of Epilepsy. Neuromodulation 2025; ■: 1–15.

#### REFERENCES

- Engel J. Epilepsy: Global Issues for the Practicing Neurologist: World Federation of Neurology, Seminars in Clincal Neurology. 2. Demos Medical Publishing; 2005.
- Savage N. Epidemiology: the complexities of epilepsy. Nature. 2014;511:S2–S3. https://doi.org/10.1038/511S2a

- 3. French JA. Refractory epilepsy: clinical overview. *Epilepsia*. 2007;48(s1 suppl 1):3–7. https://doi.org/10.1111/j.1528-1167.2007.00992.x
- Spencer SS. Neural networks in human epilepsy: evidence of and implications for treatment. *Epilepsia*. 2002;43:219–227. https://doi.org/10.1046/j.1528-1157.2002. 26901 x
- Schramm J. Temporal lobe epilepsy surgery and the quest for optimal extent of resection: a review. *Epilepsia*. 2008;49:1296–1307. https://doi.org/10.1111/j.1528-1167.2008.01604.x
- Bertram EH. Neuronal circuits in epilepsy: do they matter? Exp Neurol. 2013;244:67–74. https://doi.org/10.1016/j.expneurol.2012.01.028
- Engel J, Pitkänen A, Loeb JA, et al. Epilepsy biomarkers. Epilepsia. 2013;54(suppl 4):61–69. https://doi.org/10.1111/epi.12299
- Nelson TS, Suhr CL, Freestone DR, et al. Closed-loop seizure control with very high frequency electrical stimulation at seizure onset in the gaers model of absence epilepsy. Int J Neural Syst. 2011;21:163–173. https://doi.org/10.1142/S0129065711002717
- Sisterson ND, Wozny TA, Kokkinos V, Constantino A, Richardson RM. Closed-loop brain stimulation for drug-resistant epilepsy: towards an evidence-based approach to personalized medicine. Neurotherapeutics. 2019;16:119–127. https:// doi.org/10.1007/s13311-018-00682-4
- de Castro Medeiros D de C, Raspante LBP, Mourão FAG, Carvalho VR, Mendes EMAM, Moraes MFD. Deep brain stimulation probing performance is enhanced by pairing stimulus with epileptic seizure. *Epilepsy Behav*. 2018;88:380– 387. https://doi.org/10.1016/j.yebeh.2018.09.048
- Medeiros DC, Oliveira LB, Mourão FAG, et al. Temporal rearrangement of pre-ictal PTZ induced spike discharges by low frequency electrical stimulation to the amygdaloid complex. *Brain Stimul*. 2014;7:170–178. https://doi.org/10.1016/j.brs. 2013.11.005
- Moraes MFD, de Castro Medeiros D, Mourao FAG, Cancado SAV, Cota VR. Epilepsy as a dynamical system, a most needed paradigm shift in epileptology. *Epilepsy Behav*. 2021;121:106838. https://doi.org/10.1016/j.yebeh.2019.106838
- Pinto HPP, de Oliveira Lucas EL, Carvalho VR, et al. Seizure susceptibility corrupts inferior colliculus acoustic integration. Front Syst Neurosci. 2019;13:63. https://doi. org/10.3389/fnsys.2019.00063
- Mesquita MBS, Medeiros D de C, Cota VR, Richardson MP, Williams S, Moraes MFD.
  Distinct temporal patterns of electrical stimulation influence neural recruitment
  during PTZ infusion: an fMRI study. *Prog Biophys Mol Biol*. 2011;105:109–118.
  <a href="https://doi.org/10.1016/j.pbiomolbio.2010.10.005">https://doi.org/10.1016/j.pbiomolbio.2010.10.005</a>
- Ryulin P, Rheims S, Hirsch LJ, Sokolov A, Jehi L. Neuromodulation in epilepsy: state-of-the-art approved therapies. *Lancet Neurol.* 2021;20:1038–1047. https://doi.org/10.1016/S1474-4422(21)00300-8
- Salama H, Salama A, Oscher L, Jallo GI, Shimony N. The role of neuromodulation in the management of drug-resistant epilepsy. *Neurol Sci Off J Ital Neurol Soc Ital Soc Clin Neurophysiol*. 2024;45:4243–4268. https://doi.org/10.1007/s10072-024-07513-9 Published online April 20, 2024.
- Hauptmann C, Tass PA. Therapeutic rewiring by means of desynchronizing brain stimulation. *Biosystems*. 2007;89:173–181. https://doi.org/10.1016/j.biosystems. 2006.04.015
- Nunez PL, Srinivasan R. Electric Fields of the Brain. Oxford University Press; 2006. https://doi.org/10.1093/acprof:oso/9780195050387.001.0001
- Cota VR, Drabowski BMB, de Oliveira JC, Moraes MFD. The epileptic amygdala: toward the development of a neural prosthesis by temporally coded electrical stimulation. J Neurosci Res. 2016;94:463–485. https://doi.org/10.1002/jnr.23741
- Mourão FAG, Lockmann ALV, Castro GP, et al. Triggering different brain states using asynchronous serial communication to the rat amygdala. *Cereb Cortex*. 2016;26:1866–1877. https://doi.org/10.1093/cercor/bhu313
- Cota VR, Moraes MFD. editorial. Editorial: Engineered neuromodulation approaches to treat neurological disorders. Front Neurosci. 2022;16:1038215. https://doi.org/10.3389/fnins.2022.1038215
- Cota VR, Cançado SAV, Moraes MFD. On temporal scale-free non-periodic stimulation and its mechanisms as an infinite improbability drive of the brain's functional connectogram. Front Neuroinform. 2023;17:1173597. https://doi.org/10.3389/fninf.2023.1173597
- Sunderam S, Gluckman B, Reato D, Bikson M. Toward rational design of electrical stimulation strategies for epilepsy control. *Epilepsy Behav*. 2010;17:6–22. https://doi.org/10.1016/j.yebeh.2009.10.017
- Buzsáki G, Vöröslakos M. Brain rhythms have come of age. Neuron. 2023;111:922–926. https://doi.org/10.1016/j.neuron.2023.03.018
- Glass L. Synchronization and rhythmic processes in physiology. Nature. 2001;410:277–284. https://doi.org/10.1038/35065745
- Womelsdorf T, Schoffelen JM, Oostenveld R, et al. Modulation of neuronal interactions through neuronal synchronization. Science. 2007;316:1609–1612. https:// doi.org/10.1126/science.1139597
- Womelsdorf T, Fries P. The role of neuronal synchronization in selective attention. Curr Opin Neurobiol. 2007;17:154–160. https://doi.org/10.1016/j.conb.2007.02.002
- Kreuz T, Mormann F, Andrzejak RG, Kraskov A, Lehnertz K, Grassberger P. Measuring synchronization in coupled model systems: A comparison of different approaches. *Phys Nonlinear Phenom*. 2007;225:29–42. https://doi.org/10.1016/j. physd.2006.09.039
- Tsien JZ. Linking Hebb's coincidence-detection to memory formation. Curr Opin Neurobiol. 2000;10:266–273. https://doi.org/10.1016/S0959-4388(00)00070-2
- Fuentealba P, Steriade M. The reticular nucleus revisited: intrinsic and network properties of a thalamic pacemaker. *Prog Neurobiol*. 2005;75:125–141. https://doi. org/10.1016/i.pneurobio.2005.01.002

- Gao JX, Yan G, Li XX, et al. The ponto-Geniculo-occipital (PGO) waves in dreaming: an overview. Brain Sci. 2023;13:1350. https://doi.org/10.3390/brainsci13091350
- Steriade M. The corticothalamic system in sleep. Front Biosci. 2003;8:d878–d899. https://doi.org/10.2741/1043
- Uhlhaas PJ, Linden DEJ, Singer W, et al. Dysfunctional long-range coordination of neural activity during gestalt perception in schizophrenia. *J Neurosci*. 2006;26:8168–8175. https://doi.org/10.1523/JNEUROSCI.2002-06.2006
- Uhlhaas PJ, Singer W. Neural synchrony in brain disorders: relevance for cognitive dysfunctions and pathophysiology. *Neuron*. 2006;52:155–168. https://doi.org/10. 1016/j.neuron.2006.09.020
- 35. Avanzini G, Forcelli PA, Gale K. Are there really "epileptogenic" mechanisms or only corruptions of "normal" plasticity? *Adv Exp Med Biol.* 2014;813:95–107. https://doi.org/10.1007/978-94-017-8914-1\_8
- Doubovikov ED, Serdyukova NA, Greenberg SB, Gascoigne DA, Minhaj MM, Aksenov DP. Electric field effects on brain activity: implications for epilepsy and burst suppression. Cells. 2023;12:2229. https://doi.org/10.3390/cells12182229
- Batista Tsukahara VH, de Oliveira Júnior JN, de Oliveira Barth VB, de Oliveira JC, Rosa Cota V, Maciel CD. Data-driven network dynamical model of rat brains during acute ictogenesis. Front Neural Circuits. 2022;16:747910. https://doi.org/10.3389/ fprir. 2022.747910
- Moraes MFD, Chavali M, Mishra PK, Jobe PC, Garcia-Cairasco N. A comprehensive electrographic and behavioral analysis of generalized tonic-clonic seizures of GEPR-9s. Brain Res. 2005;1033:1–12. https://doi.org/10.1016/j.brainres.2004.10.066
- Moraes MFD, Mishra PK, Jobe PC, Garcia-Cairasco N. An electrographic analysis of the synchronous discharge patterns of GEPR-9s generalized seizures. *Brain Res.* 2005;1046:1–9. https://doi.org/10.1016/j.brainres.2005.03.035
- Browning RA. Role of the brain-stem reticular formation in tonic-clonic seizures: lesion and pharmacological studies. Fed Proc. 1985;44:2425–2431.
- Eells JB, Clough RW, Browning RA, Jobe PC. Comparative fos immunoreactivity in the brain after forebrain, brainstem, or combined seizures induced by electroshock, pentylenetetrazol, focally induced and audiogenic seizures in rats. Neuroscience. 2004;123:279–292. https://doi.org/10.1016/j.neuroscience.2003.08.015
- Li Q, Chen Y, Wei Y, et al. Functional network connectivity patterns between idiopathic generalized epilepsy with myoclonic and absence seizures. Front Comput Neurosci. 2017;11:38. https://doi.org/10.3389/fncom.2017.00038
- Brodovskaya A, Kapur J. Circuits generating secondarily generalized seizures. *Epilepsy Behav*. 2019;101:106474. https://doi.org/10.1016/j.yebeh.2019.106474
- Dabrowska N, Joshi S, Williamson J, et al. Parallel pathways of seizure generalization. Brain. 2019;142:2336–2351. https://doi.org/10.1093/brain/awz170
- Lüttjohann A, van Luijtelaar G. The role of thalamic nuclei in genetic generalized epilepsies. Epilepsy Res. 2022;182:106918. https://doi.org/10.1016/j.eplepsyres. 2022.106918
- Peng SJ, Hsin YL. Functional connectivity of the corpus callosum in epilepsy patients with secondarily generalized seizures. Front Neurol. 2017;8:446. https:// doi.org/10.3389/fneur.2017.00446
- Tyvaert L, Chassagnon S, Sadikot A, LeVan P, Dubeau F, Gotman J. Thalamic nuclei activity in idiopathic generalized epilepsy: An EEG-fMRI study. *Neurology*. 2009;73:2018–2022. https://doi.org/10.1212/WNL.0b013e3181c55d02
- Medeiros D de C, Cota VR, Vilela MRS da P, Mourão FAG, Massensini AR, Moraes MFD. Anatomically dependent anticonvulsant properties of temporallycoded electrical stimulation. *Epilepsy Behav*. 2012;23:294–297. https://doi.org/10. 1016/j.yebeh.2012.01.004
- Medeiros D de C, Moraes MFD. Focus on desynchronization rather than excitability: A new strategy for intraencephalic electrical stimulation. *Epilepsy Behav*. 2014;38:32–36. https://doi.org/10.1016/j.yebeh.2013.12.034
- de Oliveira JC de, Maciel RM, Moraes MFD, Rosa Cota VR. Asynchronous, bilateral, and biphasic temporally unstructured electrical stimulation of amygdalae enhances the suppression of pentylenetetrazole-induced seizures in rats. *Epilepsy Res.* 2018;146:1–8. https://doi.org/10.1016/j.eplepsyres.2018.07.009
- de Oliveira JC de, Medeiros D de C, de Souza E Rezende GH de Se, Moraes MFD, Cota VR. Temporally unstructured electrical stimulation to the amygdala suppresses behavioral chronic seizures of the pilocarpine animal model. *Epilepsy Behav*. 2014;36:159–164. https://doi.org/10.1016/j.yebeh.2014.05.005
- 52. de Oliveira JC de, Drabowski BMB, Rodrigues SMAF, Maciel RM, Moraes MFD, Cota VR. Seizure suppression by asynchronous non-periodic electrical stimulation of the amygdala is partially mediated by indirect desynchronization from nucleus accumbens. *Epilepsy Res.* 2019;154:107–115. https://doi.org/10.1016/j.eplepsyres. 2019.05.009
- 53. Réboli LA, Maciel RM, de Oliveira JC, Moraes MFD, Tilelli CQ, Cota VR. Persistence of neural function in animals submitted to seizure-suppressing scale-free non-periodic electrical stimulation applied to the amygdala. *Behav Brain Res.* 2022;426: 113843. https://doi.org/10.1016/j.bbr.2022.113843
- Sah P, Faber ESL, Lopez De Armentia M, Power J. The amygdaloid complex: anatomy and physiology. *Physiol Rev.* 2003;83:803–834. https://doi.org/10.1152/ physrev.00002.2003
- Benini R, D'Antuono M, Pralong E, Avoli M. Involvement of amygdala networks in epileptiform synchronization in vitro. *Neuroscience*. 2003;120:75–84. https://doi. org/10.1016/s0306-4522(03)00262-8
- Hirsch E, Danober L, Simler S, et al. The amygdala is critical for seizure propagation from brainstem to forebrain. *Neuroscience*. 1997;77:975–984. https://doi.org/10. 1016/s0306-4522(96)00503-9
- 57. Prager EM, Aroniadou-Anderjaska V, Almeida-Suhett CP, Figueiredo TH, Apland JP, Braga MFM. Acetylcholinesterase inhibition in the basolateral

- amygdala plays a key role in the induction of status epilepticus after soman exposure. *Neurotoxicology*. 2013;38:84–90. https://doi.org/10.1016/j.neuro. 2013.06.006
- Racine RJ. Modification of seizure activity by electrical stimulation: cortical areas. *Electroencephalogr Clin Neurophysiol*. 1975;38:1–12. https://doi.org/10.1016/0013-4694(75)90204-7
- Racine R, Newberry F, Burnham WM. Post-activation potentiation and the kindling phenomenon. *Electroencephalogr Clin Neurophysiol*. 1975;39:261–271. https://doi. org/10.1016/0013-4694(75)90148-0
- Cota VR, Medeiros D de C, Vilela MRS da P, Doretto MC, Moraes MFD. Distinct patterns of electrical stimulation of the basolateral amygdala influence pentylenetetrazole seizure outcome. *Epilepsy Behav*. 2009;14(suppl 1):26–31. https://doi. org/10.1016/j.yebeh.2008.09.006
- Mourão FAG, Guarnieri L de O, Amaral Júnior PAA, Carvalho VR, Mendes EMAM, Moraes MFD. A fully adapted headstage with custom electrode arrays designed for electrophysiological experiments. Front Neurosci. 2021;15:691788. https://doi. org/10.3389/fnins.2021.691788
- Gröticke I, Hoffmann K, Löscher W. Behavioral alterations in a mouse model of temporal lobe epilepsy induced by intrahippocampal injection of kainate. *Exp Neurol.* 2008;213:71–83. https://doi.org/10.1016/j.expneurol.2008.04.036
- Rattka M, Brandt C, Löscher W. The intrahippocampal kainate model of temporal lobe epilepsy revisited: epileptogenesis, behavioral and cognitive alterations, pharmacological response, and hippoccampal damage in epileptic rats. *Epilepsy Res.* 2013;103:135–152. https://doi.org/10.1016/j.eplepsyres.2012.09.015
- Chen Y. Mechanisms of winner-take-all and group selection in neuronal spiking networks. Front Comput Neurosci. 2017;11:20. https://doi.org/10.3389/fncom.2017. 2022.
- Abdallah C, Mansilla D, Minato E, Grova C, Beniczky S, Frauscher B. Systematic review of seizure-onset patterns in stereo-electroencephalography: current state and future directions. *Clin Neurophysiol*. 2024;163:112–123. https://doi.org/10. 1016/j.clinph.2024.04.016
- Di Giacomo RD, Uribe-San-Martin R, Mai R, et al. Stereo-EEG ictal/interictal patterns and underlying pathologies. Seizure. 2019;72:54–60. https://doi.org/10.1016/j.seizure.2019.10.001
- Hu L, Xiong K, Ye L, et al. Ictal EEG desynchronization during low-voltage fast activity for prediction of surgical outcomes in focal epilepsy. *J Neurosurg*. 2023;139:238–247. https://doi.org/10.3171/2022.11JNS221469
- Lu H, Yang H, Zhang W, Liu X, Sun W. An ictogenic marker in the mesial temporal epilepsy and its temporal evolutionary features. Front Neurol. 2024;15:1510108. https://doi.org/10.3389/fneur.2024.1510108
- Kim SY, Lim W. Dynamical origin for winner-take-all competition in a biological network of the hippocampal dentate gyrus. *Phys Rev E*. 2022;105:014418. https://doi.org/10.1103/PhysRevE.105.014418
- Carvalho VR, Moraes MFD, Cash SS, Mendes EMAM. Active probing to highlight approaching transitions to ictal states in coupled neural mass models. *PLoS Comput Biol Taylor PN*. 2021;17:e1008377. https://doi.org/10.1371/journal.pcbi. 1008377
- Kerr WT, McFarlane KN, Figueiredo Pucci G. The present and future of seizure detection, prediction, and forecasting with machine learning, including the future impact on clinical trials. Front Neurol. 2024;15:1425490. https://doi.org/10.3389/ fneur.2024.1425490
- Mormann F, Andrzejak RG, Elger CE, Lehnertz K. Seizure prediction: the long and winding road. *Brain*. 2007;130:314–333. https://doi.org/10.1093/brain/awl241
- Valentín A, Alarcón G, Honavar M, et al. Single pulse electrical stimulation for identification of structural abnormalities and prediction of seizure outcome after epilepsy surgery: a prospective study. *Lancet Neurol*. 2005;4:718–726. https://doi. org/10.1016/S1474-4422(05)70200-3
- Frauscher B, Bartolomei F, Baud MO, Smith RJ, Worrell G, Lundstrom BN. Stimulation to probe, excite, and inhibit the epileptic brain. *Epilepsia*. 2023;64(suppl 3):S49–S61. https://doi.org/10.1111/epi.17640
- Hariz MI, Blomstedt P, Zrinzo L. Deep brain stimulation between 1947 and 1987: the untold story. Neurosurg Focus. 2010;29:E1. https://doi.org/10.3171/2010.4. FOCUS 10106
- Benabid AL, Pollak P, Louveau A, Henry S, de Rougemont J. Combined (thalamotomy and stimulation) stereotactic surgery of the VIM thalamic nucleus for bilateral Parkinson disease. *Appl Neurophysiol.* 1987;50:344–346. https://doi.org/10.1159/000100803
- Nuttin B, Cosyns P, Demeulemeester H, Gybels J, Meyerson B. Electrical stimulation in anterior limbs of internal capsules in patients with obsessive-compulsive disorder. *Lancet.* 1999;354:1526. https://doi.org/10.1016/S0140-6736(99)02376-4
- Mayberg HS, Lozano AM, Voon V, et al. Deep brain stimulation for treatmentresistant depression. *Neuron*. 2005;45:651–660. https://doi.org/10.1016/j.neuron. 2005.02.014
- Birdno MJ, Grill WM. Mechanisms of deep brain stimulation in movement disorders as revealed by changes in stimulus frequency. *Neurotherapeutics*. 2008;5:14– 25. https://doi.org/10.1016/j.nurt.2007.10.067
- Chiken S, Nambu A. Mechanism of deep brain stimulation: Inhibition, excitation, or disruption? *Neuroscientist*. 2016;22:313–322. https://doi.org/10.1177/ 1073858415581986
- Cota VR, de Oliveira JC, Damázio LCM, Moraes MFD. Nonperiodic stimulation for the treatment of refractory epilepsy: applications, mechanisms, and novel insights. *Epilepsy Behav*. 2021;121:106609. https://doi.org/10.1016/j.yebeh.2019. 106609

#### TEMPORALLY CODED NEUROMODULATION

- 82. Tass PA. A model of desynchronizing deep brain stimulation with a demandcontrolled coordinated reset of neural subpopulations. Biol Cybern. 2003;89:81-88. https://doi.org/10.1007/s00422-003-0425-7
- 83. Tass PA. Desynchronizing double-pulse phase resetting and application to deep brain stimulation. Biol Cybern. 2001;85:343-354. https://doi.org/10.1007/s0042201
- 84. Schacter DL, Buckner RL. Priming and the brain. Neuron. 1998;20:185-195. https:// doi.org/10.1016/S0896-6273(00)80448-1
- 85. Tulving E, Schacter DL. Priming and human memory systems. Science. 1990;247:301-306. https://doi.org/10.1126/science.2296719
- 86. Kalitzin SN, Velis DN, da Silva FHL da. Stimulation-based anticipation and control of state transitions in the epileptic brain. Epilepsy Behav. 2010;17:310-323. https:// doi.org/10.1016/j.yebeh.2009.12.023
- 87. Le Duigou C, Wittner L, Danglot L, Miles R. Effects of focal injection of kainic acid into the mouse hippocampus in vitro and ex vivo. J Physiol. 2005;569:833-847. https://doi.org/10.1113/jphysiol.2005.094599

# **COMMENTS**

This manuscript evaluates the effects of temporally coded electrical stimulation applied to the AMY on seizure propagation in a KA-induced focal epilepsy rat model. The authors explore two hypotheses: 1) lowfrequency (0.5 Hz) probing stimulation of the ipsilateral AMY can serve as a predictive signal for seizure onset without affecting seizure

dynamics, and 2) temporally patterned (PS vs NPS) stimulation of the contralateral AMY affects interhemispheric seizure propagation.

The study addresses important aspects of neuromodulation, epilepsy, and seizure propagation, providing insights relevant to clinical translation and closed-loop therapeutic systems. The authors use sophisticated electrophysiologic recordings and stimulation protocols, providing multisite, bilateral measurements, and the use of temporally patterned stimulation (NPS vs PS) introduces an innovative perspective in neuromodulation strategies.

> Mohamed Rabieh Khalife, PhD Newark, DE, USA

In the present manuscript, the authors interestingly show that applying a regular oscillation and low-frequency stimulation to the ipsilateral AMY facilitated seizure propagation. However, nonrepeating and temporally complex inputs disrupted network integration, impairing seizure generalization. Therefore, applying low-frequency stimuli to the ipsilateral AMY is a suitable strategy for seizure prediction. Javad Mirnajafi-Zadeh, PhD

Tehran, Iran